$Mn_{0.9}Co_{0.1}P$ in an external field: Lifshitz point and irreversibility behavior of disordered incommensurate phases

A. Zięba
Department of Physics and Nuclear Techniques, Academy of Mining and Metallurgy, 30039 Krakow, Poland

C. C. Becerra
Institute of Physics, University of São Paulo, São Paulo, Brazil

H. Fjellvåg
Department of Chemistry, University of Oslo, N-0315 Oslo 3, Norway

N. F. Oliveira, Jr.
Institute of Physics, University of São Paulo, São Paulo, Brazil

A. Kjekshus
Department of Chemistry, University of Oslo, N-0315 Oslo 3, Norway
(Received 11 December 1991)

A single crystal of $Mn_{0.9}Co_{0.1}P$, which represents a homolog of MnP with disorder on the metal sublattice, has been studied by use of ac susceptibility and magnetization measurements in order to investigate the effects of randomness on its incommensurate magnetic phases and magnetic phase transitions. Detailed results are given for $T > 1.7$ K and external field $H \leq 70$ kOe applied along the orthorhombic b axis ($a > b > c$). The high-temperature part of the phase diagram for $\mathbf{H}\|\mathbf{b}$, is qualitatively similar to that of pure MnP, and includes a Lifshitz point on the confluence of the paramagnetic (P), ferromagnetic (F), and modulated fanlike magnetic phases. The derived crossover exponent is unchanged or just slightly larger than that of MnP. The exponent characterizing the magnetization discontinuity along the F–fan line is $\tilde{\beta} \approx 0.5$. All first-order transitions show hysteresis (being negligible or small in MnP). The transition between the incommensurate screw and fan phases, occurs via a few steps on increasing field ($\mathbf{H}\|\mathbf{b}$), and with a Barkhausen-like noise on decreasing field. Irreversible behavior occurs also *inside* the entire region of the fan phase. The second-order fan–P transition line $H_{\lambda *}(T)$, which, in MnP, is observed down to zero temperature, fades away at about 10 K in $Mn_{0.9}Co_{0.1}P$. The domain of irreversible behavior extends up to the irreversibility line $H_{irr}(T) > H_{\lambda *}(T)$, with $H_{irr}(T)$ sharply increasing at low temperatures.

I. INTRODUCTION

Manganese monophosphide (MnP) is an orthorhombic metallic compound. Because of the richness of its magnetically ordered (in particular incommensurate) phases and magnetic phase transitions, it is often considered as a model substance in phase-transition physics. In fact, MnP is the only magnetic system for which a Lifshitz multicritical point has been observed, and several critical exponents have been determined.[1–7]

Frozen disorder is considered a relevant factor for changing the characteristics of the ordered phases and phase transformations. The disorder creates (in terms of microscopic models) random exchange and random anisotropy and may, in nonzero external field, lead to random fields.[8] The effects of randomness have experimentally been studied during the last decade, mostly in ferromagnets[9,10] and antiferromagnets.[11,12] However, very little experimental data have been obtained for disordered incommensurate phases. Hence detailed experiments on a properly disordered homolog of MnP seems rewarding. This is done in the present work through the study of the magnetic properties of a $Mn_{0.9}Co_{0.1}P$ single crystal.

A. Main features of the magnetic phase diagrams of MnP

Two magnetically ordered phases occur for MnP in zero field, respectively, a ferromagnetic (F) phase existing between $T_C = 291$ K and $T_S = 47$ K (Ref. 13) and a helimagnetic phase of the double-screw type (later simply labeled "screw") below T_S.[14] The character of the magnetic phases, both in zero and nonzero fields, is influenced by the orthorhombic magnetocrystalline anisotropy. It directs the magnetization vector of the ferromagnetic phase, in the absence of a field, along the "easy" c axis. (The notation for the axes $a > b > c$ is used here in accordance with earlier publications on the phase transitions in MnP, which implies the *Pncm* nonstandard setting of the crystallographic unit cell.) In MnP, b is the intermediate-anisotropy axis and a is the hard-anisotropy axis. In order to minimize the anisotropy energy, the

magnetic moments of the screw phase rotate in the *bc* plane, with some bunching along the easy *c* axis.[15]

The magnetic phase diagram obtained for the magnetic field **H**||**c** (i.e., along the easy direction) is shown in the upper part of Fig. 1. In this case the ferromagnetic phase exists only for $H=0$, $T_S<T<T_C$, and the phase boundary between the screw ($T<T_S$) and paramagnetic (P) phases is first order. The critical exponents β, γ, and δ for the $F-P$ transition have been determined by Terui, Komatsubara, and Hirahara.[16]

If the magnetic field is applied along the intermediate axis (**H**||**b**), another modulated magnetic structure, the fan phase, is observed in addition to the others, just mentioned, screw, F, and P phases (Fig. 1). The **H**||**b** phase diagram exhibits two points where three distinct phases meet. The screw–F–fan triple point is a classical triple point with three first-order phase boundaries crossing at sharp angles. On the contrary, the F–fan–P point is the first, and the most thoroughly studied, experimental example of a Lifshitz multicritical point (LP). For this LP three exponents have been experimentally determined, viz., the crossover exponent ϕ,[1,2,5] the spiral propagation vector exponent $\tilde{\beta}_k$,[4] and the specific-heat exponent α_L.[5–7]

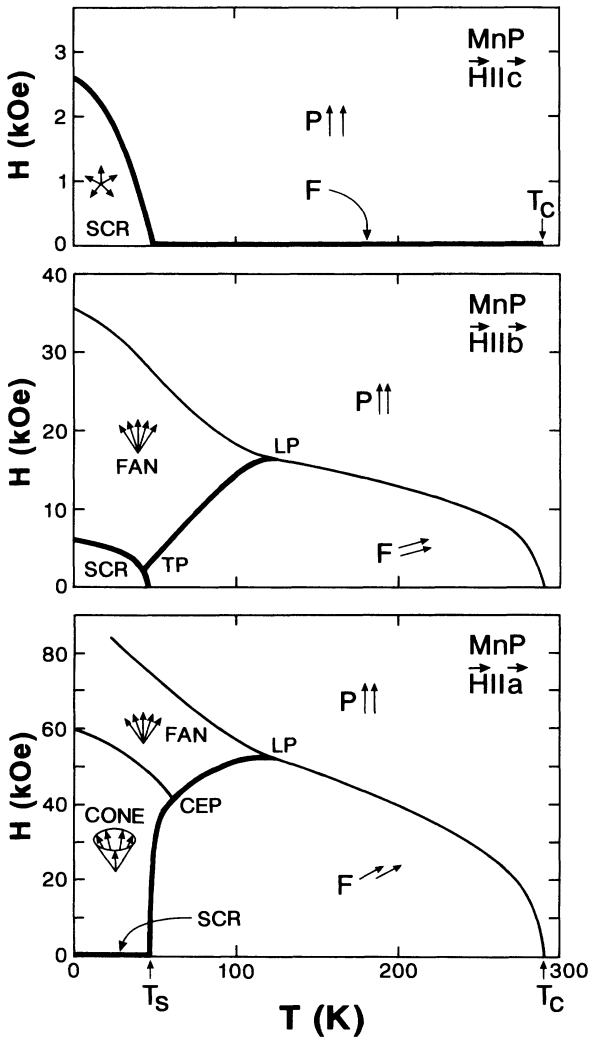

FIG. 1. Magnetic phase diagrams for MnP for external fields along the three principal crystallographic axes (from Refs. 1, 6, and 13). Magnetic states are indicated by P (para, spin aligned), F (ferro), SCR (screw), CONE (cone), and FAN (fan); T_C denotes the Curie temperature, T_S the screw–F transition, CEP the critical end point, TP the triple point, and LP the Lifshitz point.

The magnetic phase diagram for the hard direction, **H**||**a**, looks somewhat similar to that for **H**||**b**, with the region of the screw phase replaced by a cone spin structure (Fig. 1). The transition fields to the P phase are, because of higher anisotropy, substantially larger than in the corresponding **H**||**b** diagram. The F–fan–P "triple point" is again a Lifshitz point.[3] One major difference occurs as a result of the second-order character of the cone–fan transition. Consequently, the F–cone–fan confluence point is a critical end point (CEP).[17]

Phase diagrams, for external-field directions within the *ab* plane, are presently being explored at the University of São Paulo. In particular, both LP's mentioned above form in the H_a-H_b-T space a line of Lifshitz points.[18] When the external-field direction is not exactly confined within the *ab* plane, the $F-P$ transition gets smeared (the F phase no longer exists except for $H=0$). This property is used experimentally to facilitate proper alignment of the crystal with respect to the magnetic field.

B. Substituted manganese monophosphide systems: The properties of $Mn_{1-\ell}Co_\ell P$

The crystal structure of MnP allows substitution of both Mn and P atoms by other elements with similar chemical properties. Magnetic composition–temperature phase diagrams have been determined for several $Mn_{1-\ell}\mathcal{T}_\ell P$ (metal sublattice) solid-solution systems [$\mathcal{T}$=V,Cr,[19,20] Fe,Co,[20] and Ni,Mo,W[21]]. Substitution of Mn atoms by $\mathcal{T}$ elements decreases in general the Curie temperature. This decrease is found to be roughly proportional to the absolute difference in the number of valence electrons[20,21] between solute and solvent. On the other hand, no simple systematics exist for the T_S transition. T_S decreases for $\mathcal{T}$=Cr and Ni, whereas it increases for the other elements. For low levels of Co substitution, T_S stays approximately constant.[20] $Mn_{1-\ell}Co_\ell P$ was hence considered as the most promising solid-solution system for which there will be only small changes in the temperature coordinate of the presumed Lifshitz point. The T-ℓ phase diagram for powder samples of $Mn_{1-\ell}Co_\ell P$ is shown in Fig. 2. Neutron-diffraction measurements for these powder samples showed an intriguing weak temperature dependence of the propagation vector of the screw phase, in marked contrast with that for MnP.[22]

No experimental data or theoretical calculations are available concerning the electronic state of the randomly distributed Co atoms in $Mn_{1-\ell}Co_\ell P$. One may speculate that the Co atoms act as approximately nonmagnetic dilutants because CoP itself is a Pauli paramagnet,[22] and a spin-glass state, presumably based on Mn atoms, occurs for $\ell \gtrsim 0.3$.[20] If so, this would in the localized-moment

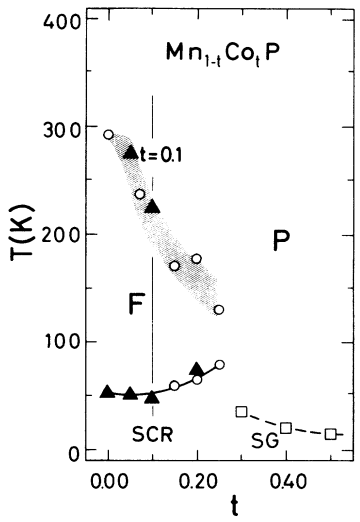

FIG. 2. Temperature–composition phase diagram for polycrystalline $Mn_{1-t}Co_tP$ (from Ref. 20). SG denotes the spin-glass region.

picture correspond to the random-site dilution model. The rather narrow domain with ordered magnetism ($0.00 \leq t \leq 0.25$) in $Mn_{1-t}Co_tP$ may be a result of competing exchange interactions, which, on the other hand, also are necessary for the presence of the incommensurate magnetic structures.

The present paper reports on various features of an $Mn_{0.9}Co_{0.1}P$ single crystal as investigated by ac susceptibility under a constant external magnetic field. Some data were obtained by magnetization measurements under a constant field and others by the pulse magnetic-field technique. The information concerning the sample and experimental techniques is given in Sec. II. Section III reports on the screw–P transition for **H**||**c**. The two main parts of the paper concern **H**||**b** (i.e., the external field along the intermediate direction). Section IV deals with the phase transitions in the vicinity of the Lifshitz point. In particular, it reports on the determination of the exponent β for the diminishing magnetization discontinuity along the F–fan phase boundary, as well as on the possible change of the crossover exponent ϕ for $Mn_{0.9}Co_{0.1}P$ in comparison with MnP. Section V deals with various aspects of irreversibility behavior, which occurs for the modulated phases at low temperatures. The irreversibility behavior inside the fan phase area, and the discovery of an irreversibility line which replaces the classical second-order fan–P boundary for $T \rightarrow 0$, has earlier been the subject of a short paper.[23] The present paper provides additional data and a detailed discussion of the effect of dilution on the modulated phases and phase transitions.

Preliminary results for **H**||**a** (i.e., parallel to the hard direction) have been previously presented.[24] Those results confirmed that for any direction of the external field, sizable hysteresis develops for all first-order transitions. The phase diagram for **H**||**a** is qualitatively similar to that reported for MnP, including the presence of a LP. Irreversibility behavior develops also for the cone phase, with an "inverse" hysteresis at the cone–fan transition. Further details are planned to be published in a forthcoming paper.[25]

II. EXPERIMENTS AND SAMPLE

The examined single crystal of $Mn_{0.9}Co_{0.1}P$ was obtained by the Bridgman method as described in Ref. 26. The measurements were performed on a 41-mm^3 cubic sample cut along the principal crystallographic axes.

X-ray-diffraction studies on smaller single crystals of $Mn_{1-t}Co_tP$ showed no signs of any long- or short-range ordering of the Co and Mn atoms. This was furthermore confirmed by neutron-diffraction studies of powder samples. Hence it is reasonable to conclude that Mn and Co are randomly distributed over the metal sublattice. The possibility of macroscopic concentration gradients was checked by performing x-ray-fluorescence scans on the different faces of the cube sample. No change in the [Mn]:[Co] ratio was observed within the 1.5% accuracy of the applied method.

For estimation of demagnetization effects, a demagnetizing factor of $\frac{1}{3}$, i.e., the same as for a sphere, was used. The nonspherical sample shape may, however, produce inhomogeneities in the internal field. This may lead to some smearing of the phase transitions measured in a homogeneous external field. This aspect was experimentally checked by cutting the corners of the cube after completing the measurements. (This operation reduced the sample mass from 252 to 206 mg.) No clear improvement in the quality of the $\chi(H)$ curves was found, and hence the cube was considered for the present experiments to be as good as a sphere, being, however, more easy to handle.

The ac susceptibility measurements under a constant field were performed in São Paulo using the experimental setup described in Ref. 3. The real (χ') and imaginary (χ'') parts of the longitudinal ac susceptibility were measured simultaneously. The modulation field, typically 4.5 Oe, 170 Hz, was applied along the external constant field. Almost all runs were made at fixed temperature by varying the field (up to 65 kOe) at a slow rate between 35 and 140 Oe/s. The sample was aligned with respect to the external field (estimated accuracy $< 0.2°$) by tuning the sharpness of the F–P transition (as described in Refs. 2 and 3).

The real part of the susceptibility is proportional to the derivative of the bulk magnetization, $\chi'(H) \propto dM(H)/dH$. The derivative character of the $\chi'(H)$ signal ensures a more precise localization of both first- and second-order transitions than the $M(H)$ curve alone. Moreover, the imaginary component $\chi''(H)$, which reflects dissipation of energy, provides additional information concerning the transition order.[17] However, for the first-order transitions in $Mn_{0.9}Co_{0.1}P$, the $\chi'(H)$ curves show no distinct peaks, as can be expected for $M(H)$ discontinuities. This occurs because the modulation field (of a few Oe) in this case is smaller than the width of the hysteresis of the transition, and the sample magnetization (in the ac field) follows a sequence of

minor hysteresis loops whose inclination is not directly related to the slope of the $M(H)$ curve.

The magnetization jump for the first-order F–fan transition was measured by a pulse-field magnetometer, which was also used earlier for the introductory examination of the $Mn_{0.9}Co_{0.1}P$ single crystal.[26] A liquid-nitrogen bath kept under 0.1–3 atm pressure was used to ensure good temperature control.[27] The magnetization measurements under a constant field were performed using a vibrating-sample magnetometer with a superconducting magnet.

III. PHASE TRANSITIONS FOR A FIELD PARALLEL TO THE EASY DIRECTION (H||c)

Application of a magnetic field parallel to the easy direction in MnP (H||c) introduces a first-order screw–P transition with a magnetization discontinuity almost matching the saturation moment.[13] The ac susceptibility data shown in Fig. 3 suggest that the same transition occurs for $Mn_{0.9}Co_{0.1}P$. At the limit $T \to 0$ the transition fields are ~2.6 kOe for MnP (Ref. 13) and ~2.3 kOe for $Mn_{0.9}Co_{0.1}P$ (for increasing field conditions). The demagnetization effect causes the screw–P transition to start at $H_{S,i}$ and to be completed at $H'_{S,i}$ (Fig. 3). The expected magnetization jump is about $1.0\mu_B$,[20] corresponding to a 1.7-kOe demagnetization field. This estimate is consistent with the measured transition spread.

Under decreasing fields, the P–screw transition spreads over the interval $H_{S,d}$ to $H'_{S,d}$ (Fig. 3). The hysteresis width at 4.2 K is 1.14 kOe. A sketch of the low-temperature part of the magnetic phase diagram for the easy direction of $Mn_{0.9}Co_{0.1}P$ is shown in the inset to Fig. 3. Because of the small magnetization of the screw phase, the transition fields $H_{S,i}$ and $H_{S,d}$ correspond approximately to the true internal fields. The appearance of a large hysteresis seems to be the only remarkable difference with respect to MnP, where it also exists, but being quite small.[28]

Two previously observed features which do not occur in pure MnP were observed in the zero-field ac susceptibility. First, a deep minimum in the susceptibility is noted at about $0.9T_C$, which in turn leads to a pronounced peak near T_C (see Fig. 2 in Ref. 26). Second, there is a large decrease of $\chi'(T)$ inside the F region starting well above the screw–F transition. The decrease in zero-field susceptibility of the F phase on approaching the first-order screw–F transition occurs only in small fields and seems to be a novel feature for the disordered system. (Similar observations have earlier been made for polycrystalline samples.[20,21]) A constant-bias field applied in any direction restores the sharpness of the $\chi'(T)$ curves.

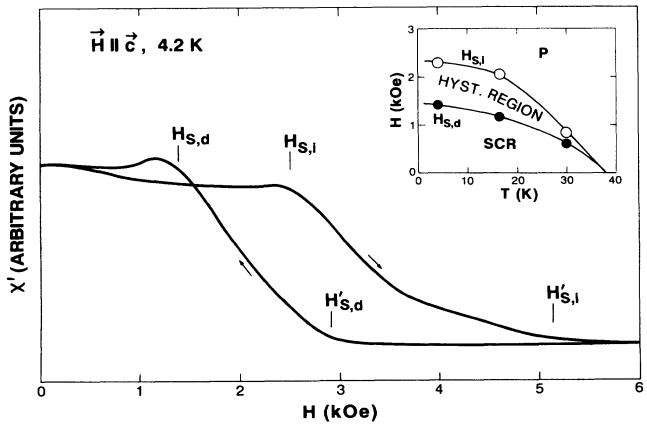

FIG. 3. Susceptibility $\chi'(H)$ curve at 42. K for external field H||c, swept up and down through the screw–P transition. The inset shows the corresponding phase diagram.

IV. PHASE TRANSITIONS FOR A FIELD PARALLEL TO THE INTERMEDIATE DIRECTION (H||b): THE LIFSHITZ POINT

A. Phase diagram near the Lifshitz point

The global phase diagram (from Ref. 23) for $Mn_{0.9}Co_{0.1}P$ for the most extensively studied field direction H||b is shown in Fig. 4 in order to facilitate the discussion of its individual regions. The high-temperature part of Fig. 4 is qualitatively similar to the corresponding diagram for MnP. However, the characteristic temperatures and magnetic fields are scaled down. Representative susceptibility curves near the F–fan–P point are shown in Fig. 5. For $T \geq 100$ K, the susceptibility of the F phase increases only slightly with increasing applied field up to the critical field H_λ, whereafter it falls to a low

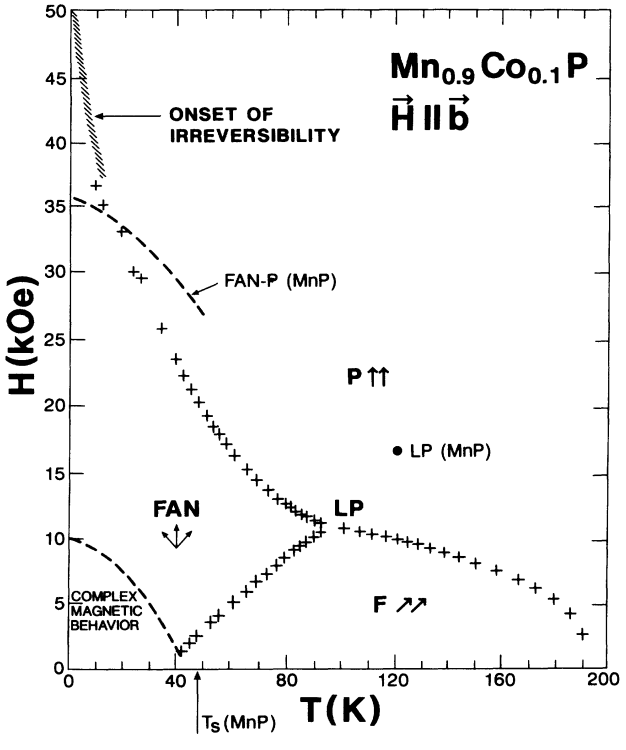

FIG. 4. Global magnetic phase diagram for $Mn_{0.9}Co_{0.1}P$ (H||b) (from Ref. 23 with slight modifications). The locations of the LP, T_S, and F–fan line (dashed curve) for MnP are included for comparison.

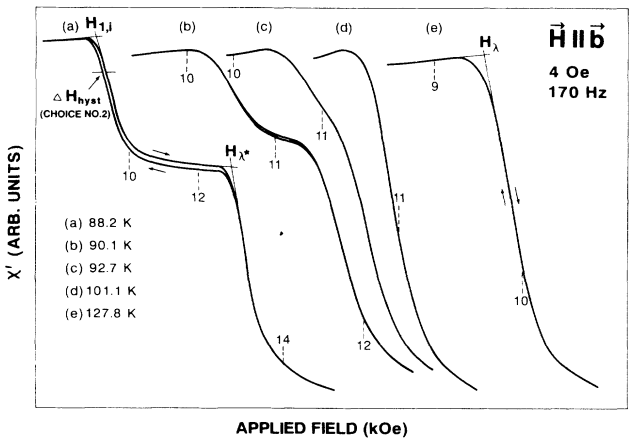

FIG. 5. Selected susceptibility traces $\chi'(H)$ ($\mathbf{H}\|\mathbf{b}$) at temperatures given in the illustration. Curves (a) below T_L and (e) above T_L show the way of deducing transition fields. Curves (b)–(d) show $\chi'(H)$ in the vicinity of LP. The curves are shifted horizontally for clarity; field scale markers (in kOe) are given for each curve. Note that the field scale for curve (a) is half the others.

value characteristic of the P phase. At lower temperatures the transition to the P phase occurs in two steps, and the corresponding fields are denoted H_1 and H_{λ^*}. The phase intersecting the F and P regions is, in analogy with MnP, interpreted as the fan phase. The transitions appear more smeared than those observed for MnP. The transition fields were determined by the intersection of tangents to the $\chi'(T)$ curve somewhat arbitrarily selected just below and above the transition (Fig. 5).

A qualitative difference with respect to the situation in MnP is the occurrence of an appreciable hysteresis at the F–fan transition. The corresponding transition field H_1 must accordingly be specified as $H_{1,i}$ and $H_{1,d}$ for increasing and decreasing field conditions, respectively. More remarkably, the data in Fig. 5 suggest that this hysteresis originates, at least in part, from the irreversible behavior of the very fan phase, as testified by its different susceptibility for increasing and decreasing fields (see Sec. V B).

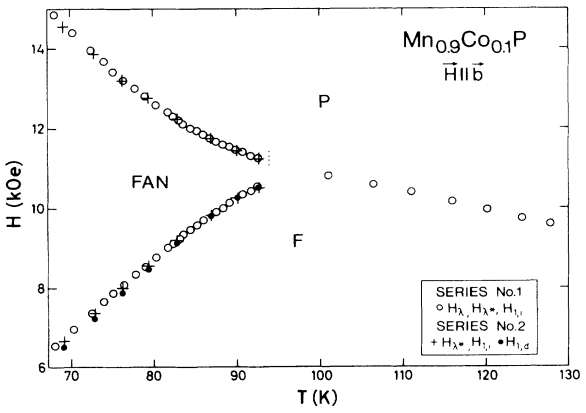

FIG. 6. Phase diagram near the LP ($\mathbf{H}\|\mathbf{b}$). Specification of symbols is given in the illustration.

The most relevant part of the phase diagram for the analysis of LP properties is shown in Fig. 6. This illustration contains data from two measurement series. Series No. 1 contains data for runs recorded for increasing fields, with temperature successively stabilized at lower values (within 0.2 K). For series No. 2 (done 2 weeks later), $\chi'(H)$ was recorded for increasing and decreasing fields to resolve the hysteresis of the F–fan transition, and the temperature was increased in steps. The values of H_{λ^*} and H_1 were extracted up to 92.7 K; however, even up to ~95 K (the dotted vertical line in Fig. 6), the occurrence of two transitions can still be seen in $\chi'(H)$. This provides the lower limit for the temperature coordinate of the LP.

B. Crossover exponent in $Mn_{0.9}Co_{0.1}P$: Comparison with MnP

The thermodynamic quantities near multicritical points are described by the extended scaling theory in terms of two scaling variables $\tilde{t}$ and $\tilde{p}$.[28] The phase boundaries are given by

$$\tilde{t}=B_i\tilde{p}^{1/\phi}\ , \tag{1}$$

where ϕ is the crossover exponent and B_i's are the amplitudes which are different for each of the i phase boundaries.

To make use of Eq. (1), a local coordinate system $\tilde{t}$, $\tilde{p}$ is defined in the T,H plane, centered at the Lifshitz point at T_L,H_L. The direction of the $\tilde{p}$ axis is uniquely determined as tangent to the phase boundaries. The direction choice for the $\tilde{t}$ axis is arbitrary as long as the asymptotic behavior is concerned, but an optimal choice extends the range of validity of the scaling laws.

The crossover exponent ϕ was determined from magnetic-phase-diagram data according to the method applied by Shapira *et al.*[2] for MnP. The method is based on the simplifying assumption that the $\tilde{t}$ axis is parallel to the H axis of the $H-T$ phase diagram. The data on the H_1 and H_{λ^*} phase boundaries are then fitted according to the formula

$$H_{\lambda^*}-H_1=B^*(T_L-T)^{1/\phi}\ , \tag{2}$$

with B^*, T_L, and ϕ as fitting parameters. The power-law fit to the *difference* $H_{\lambda^*}-H_1$ reduces the number of fitting parameters to a minimum. In particular, it is not necessary to introduce the inclination of the scaling axis $\tilde{p}$ or the field coordinate H_L for the LP.

All experimental points for increasing field (series Nos. 1 and 2) were treated as one set since these two series are quite consistent. Fits to Eq. (2) using different fitting ranges show that one can obtain stochastic distribution of the individual deviations by limiting the fitting range to 72 K. For that fitting range, which comprises 31 experimental points and corresponds to about one decade, $0.03<p<0.25$, in the relative coordinate $p=(T-T_L)/T_L$, one obtains $\phi=0.641(12)$,

$T_L = 99.0(3)$ K, and $B^* = 0.040(4)$ kOe $K^{-\phi}$.

It should be noted that uncertainty introduced by systematic errors may be larger than the calculated standard deviations (in parentheses). A particular systematic error, which is most difficult to estimate, concerns the reliability of the adopted method for determination of the transition fields. Another possible error, which is specific to $Mn_{0.9}Co_{0.1}P$, may result from the hysteresis of the F–fan transition. It appears, however (see Sec. IV C), that the hysteresis width is governed by a power law with a similar exponent, and hence the choice between $H_{1,i}$ and $H_{1,d}$ should be irrelevant. [A fit to seven points for series No. 2 using $H_{1,i}$ values gives $\phi = 0.643(21)$, whereas, using $H_{1,d}$, $\phi = 0.644(24)$ is obtained.] Finally, the external magnetic fields without any demagnetization correction were used in the analyses. Shapira *et al.*[2] argue that such a neglect should not affect ϕ by more than 0.01. A final estimate for the crossover exponent in $Mn_{0.9}Co_{0.1}P$ is $\phi = 0.64 \pm 0.04$ for the fitting range $0.03 < p < 0.25$.

The obtained values for the crossover exponent may be affected by the choice for the $\tilde{t}$ scaling axis.[29] However, the *same* procedures as in Refs. 1–3 and 5 were followed in order to facilitate a reliable comparison between the ϕ values for $Mn_{0.9}Co_{0.1}P$ and MnP. Shapira *et al.*[2] obtained 0.63 ± 0.04 for the fitting range $p < 0.35$. More recently, Bindilatti[5] obtained, for a more favorable sample shape (sphere instead of rectangular parallelepiped) and smaller ranges of the p variable, 0.605(17) for $p < 0.21$ and 0.596(32) for $p < 0.13$. Considering the errors, it is concluded that, within the limits of error, the crossover exponent for $Mn_{0.9}Co_{0.1}P$ is the same or just slightly larger than for MnP.

C. Magnetization discontinuity and hysteresis of F–fan phase boundary

The first-order characteristics of a discontinuous transition have to decrease continuously to zero on approaching any multicritical point. The application of power laws for the temperature dependence of the magnetization jump,

$$\Delta M \propto (T_L - T)^{\beta} \tag{3}$$

(with an analogous expression for the hysteresis width), is at least a natural way for parametrization of experimental data.

The magnetization discontinuity for the F–fan transition in the vicinity of the LP has not been measured for pure MnP. As discussed in Sec. II, the ac susceptibility method cannot establish the correct dM/dt in the region of the first-order transition. It is also difficult to derive accurate values of ΔM from dc magnetization curves (Fig. 7) because of uncertainties involved in extrapolation procedures. (The susceptibility of the fan phase is strongly field dependent, and so one cannot perform a linear extrapolation.) In spite of its shortcomings, the pulse-field method brings about the most reliable data for the magnetization jump in close vicinity to the LP where the value of ΔM becomes well below 1 emu/g. Because of the differential character of the primary signal dM/dt

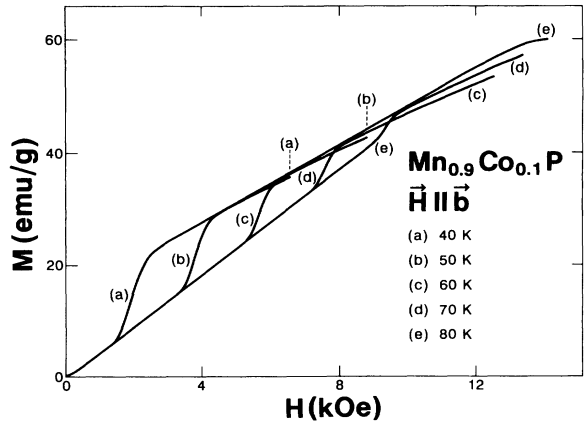

FIG. 7. Selected magnetization curves $M(H)$ ($\mathbf{H} \| \mathbf{b}$) at different temperatures, which show a F–fan discontinuous transition.

($\approx dM/dH$), ΔM can be extracted as the area under the dM/dt peak. This is shown in the inset to Fig. 8. (Examples of complete dM/dt curves are given in Ref. 26.) The estimates of ΔM for $T \geq 90$ K become gradually more uncertain because the vanishing peak of the F–fan transition is merged with the smeared λ anomaly of the critical line (compare the curves for 90 and 100.5 K in the inset to Fig. 8, the peak being distinguishable up to about 94 K).

Figure 8 shows the resulting plots for ΔM vs T and $(\Delta M)^{1/2}$ vs T. The approximately linear character of $[\Delta M(T)]^{1/2}$ for $T > 80$ K testifies to the fact that, on ap-

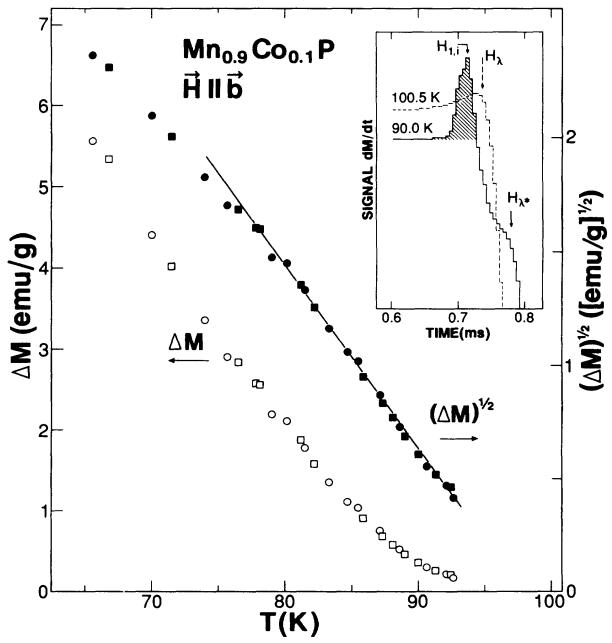

FIG. 8. Magnetization discontinuity ΔM and its square root $(\Delta M)^{1/2}$ for the F–fan transition as a function of temperature ($\mathbf{H} \| \mathbf{b}$). Circles and squares correspond to two measurement series. The inset shows how ΔM is derived from primary pulse-field signals.

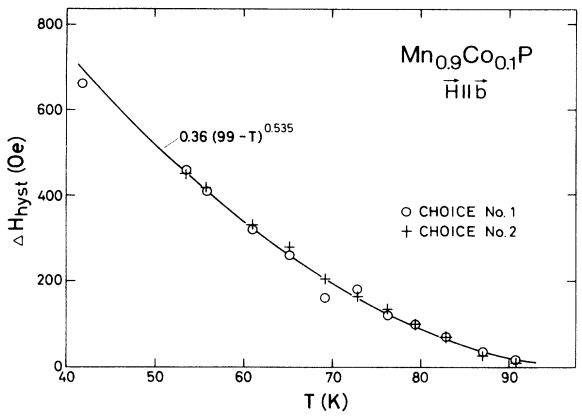

FIG. 9. Hysteresis width $H_{1,i}-H_{1,d}$ of the F-fan transition as function of temperature ($\mathbf{H}\|\mathbf{b}$). The solid line shows an example of a least-squares fit to the data, two points excluded. Concerning choice Nos. 1 and 2, see Fig. 5 and text.

proaching the LP, the vanishing of ΔM can be described by a power law with the exponent $\tilde{\beta}=0.5\pm0.05$.

The data for the hysteresis width, $\Delta H_{\rm hyst}=H_{1,i}-H_{1,d}$, are shown in Fig. 9. The values of $\Delta H_{\rm hyst}$ were either determined by subtracting $H_{1,d}$ from $H_{1,i}$ (both determined by the tangent method, choice No. 1) or were read out directly from the $\chi'(H)$ scans (as shown in Fig. 5, choice No. 2). In the region $T>\sim72$ K, the dependence $\Delta H_{\rm hyst}(T)$ can be described by a power law with an exponent between 0.5 and 0.6, depending on the fitting range and data set chosen.

D. Discussion

The work of Hornreich, Luban and Shtrikman[30] stimulated the rapid development of the modern theory of the LP in homogeneous systems. The universality class of the Lifshitz point in MnP is characterized by the space dimension $d=3$, the order parameter dimension $n=1$, and the wave-vector instability dimension $m=1$.[1,2] The comparison of the experimental exponents for pure MnP with the theoretical predictions are discussed in Refs. 1–7.

We are not aware of any theoretical predictions concerning LP's in systems with frozen disorder. According to the Harris criterion,[31] the random exchange influences the critical behavior only when the specific-heat exponent is positive. Since the value of α_L in pure Lifshitz systems is large and positive,[6] one may expect, in analogy to the random-exchange Ising model, that α_L should decrease as a result of disorder.[32] The specific-heat and crossover exponents are related by scaling laws[6,7] [up to the first-order ε expansion according to the relation $2-\alpha_L=\phi(d-m/2)$]. The decrease in α_L should bring about an *increase* in ϕ. The experimental results are inconclusive, since they bring about a small increase in ϕ, which is also consistent with an unchanged ϕ within experimental error.

Theoretical predictions concerning a first-order boundary terminated in a LP are given only within the mean-field approximation (MFA). The exponent $\tilde{\beta}=\frac{1}{2}$ was calculated by Yokoi, Coutinho-Filho, and Salinas,[33] and the present measurements represent a confirmation of this prediction.

The hysteresis is in principle a nonuniversal quantity because the first-order transition occurs before reaching the stability limit of the (old) phase. The stability limits for the first-order transition in the uniaxial LP were calculated within the MFA by Michelson,[34] who obtained $\phi=\frac{1}{2}$ for both overheating and undercooling. Recent results for the first-order spin-flop transition in the disordered systems, $K_2Fe(Cl_{1-x}Br_x)_5\cdot H_2O$ (Ref. 35) and $K_2Fe_{1-x}In_xCl_5\cdot H_2O$ (Ref. 36) show that hystereses occur, contrary to the lack of hysteresis in the corresponding pure compounds. This is similar to what is occurring in MnP where a very small hysteresis is found in the pure compound, but a significant one in the disordered system. Reference 35 explains this phenomenon in terms of inhibition of nucleation processes by pinning in the disordered system.

V. PHASE TRANSITIONS FOR A FIELD PARALLEL TO THE INTERMEDIATE DIRECTION ($\mathbf{H}\|\mathbf{b}$): IRREVERSIBILITY PHENOMENA AT LOW TEMPERATURES

A. Screw–fan transitions

All first-order transitions in $Mn_{0.9}Co_{0.1}P$, for any direction of the magnetic field, reveal some kind of hysteresis. Of these, the hysteresis behavior of the screw–fan transition appears particularly complex.

Figure 10 shows the real (χ') and imaginary (χ'') components of the longitudinal susceptibility as a function of applied field at 4.2 K. On increasing the field, $\chi'(H)$ varies in a steplike manner before reaching the characteristics of the fan phase. The corresponding $\chi''(H)$ components shows three distinct peaks (Fig. 10), labeled H_α, H_β, and H_γ. Since energy dissipation occurs for a first-order transition, it seems possible that the transition to the fan state occurs via two additional phases on (and only on) the increasing field (one existing between H_α and H_β and one between H_β and H_γ). The $\chi'(H)$ curve in Fig. 10 suggests, on the other hand, that the transition into the fan phase at H_γ occurs, with a χ' value characteristic of the fan phase, as observed for decreasing-field conditions. On further field increase, χ' first follows a part of a fan-phase minor hysteresis loop (as will be discussed in Sec. V B), and then at H_δ joins the $\chi'(H)$ curve characteristic of the field-increasing fan phase.

On decreasing-field conditions, the transition from the fan to the screw phase shows a completely different behavior. The fan phase is, for decreasing-field conditions, preserved down to a quite low field H_ε without the presence of any precursor effecting the susceptibility prior to the fan–screw transition. Then the transition to the initial screw state occurs quite violently, with a noisy, irreproducible behavior in both χ' and χ''. Figure 11 illustrates this behavior for $\chi''(H)$.

The steplike character of the screw→fan transition is

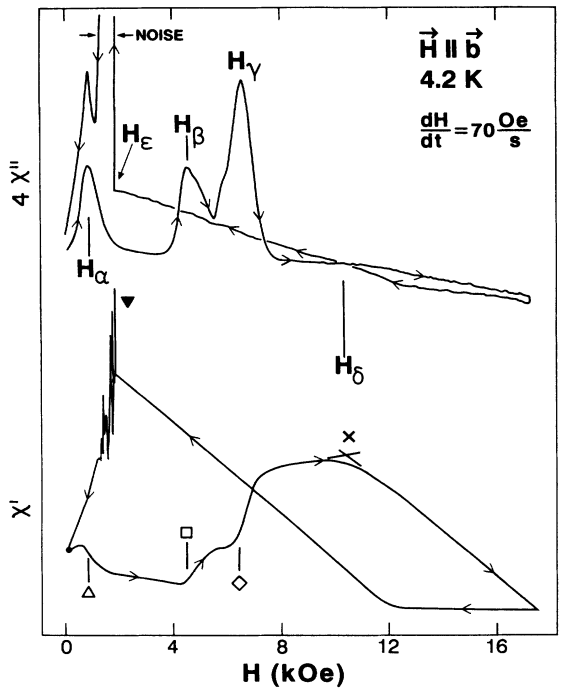

FIG. 10. Real and imaginary components of susceptibility in the screw–fan transition region at 4.2 K (**H**‖**b**). The scale for $\chi''(H)$ is 4× that for $\chi'(H)$. The symbols on $\chi'(H)$, denoting characteristic changes, correspond to points marked in Fig. 13.

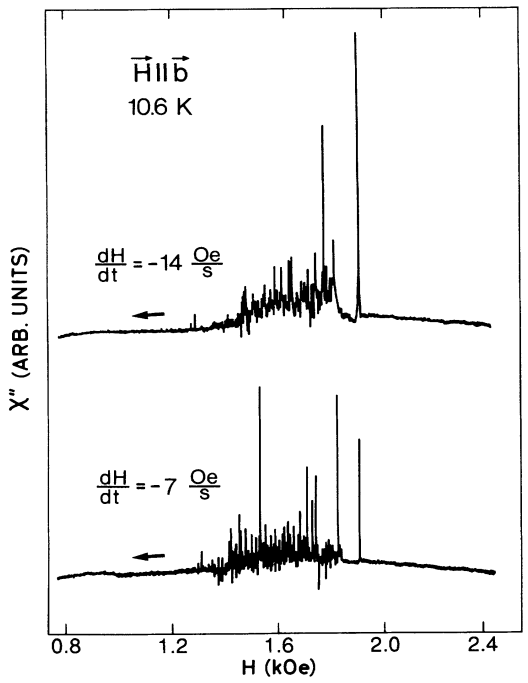

FIG. 11. Traces of $\chi''(H)$ on a decreasing field for two runs at 10.6 K, recorded with different sweep rates dH/dt in the region of the noisy fan→screw transition (**H**‖**b**).

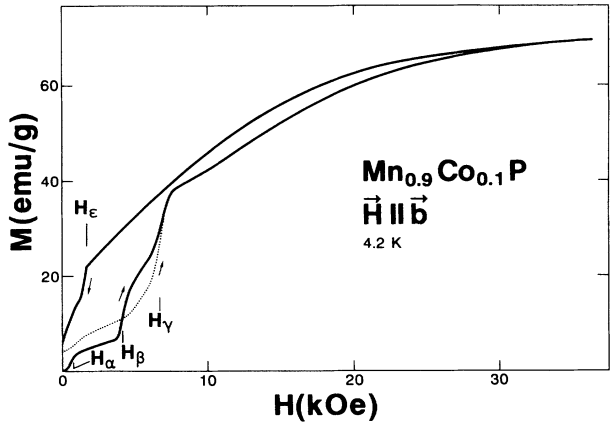

FIG. 12. Magnetization traces at 4.2 K (**H**‖**b**). The solid curve corresponds to field sweeps up and down for the "virgin" sample (i.e., cooled in zero field). The dotted curve shows the subsequent sweep "up."

further confirmed by magnetization measurements (Fig. 12). Note that after the first cycle, starting from an unmagnetized sample, a residual magnetization of about 4 emu/g is obtained in zero field. Consequently, the subsequent magnetization process in increasing fields progresses somewhat differently, as seen for $M(H)$ in Fig. 12.

The temperature dependences of the various characteristic fields discussed above are shown in Fig. 13, together with the transition field for the F–fan boundary at high temperatures. On comparison of these curves, the zero-field F–screw transition temperature is determined as $T_{S,d}=36.5\pm0.5$ K. The F–screw–fan triple point is not well defined because in the vicinity of T_S any of the three phases may be stable because of the overlapping hysteresis regions.

The structure of the possible intermediate phases (for increasing field) can be elucidated only by neutron

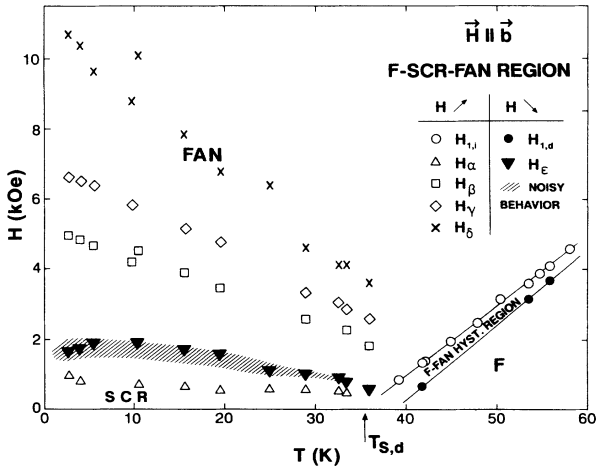

FIG. 13. "Phase diagram" for the F–screw–fan transition region (**H**‖**b**). Specification of symbols is given in the illustration; corresponding labels are also marked in Fig. 10.

diffraction. One possibility can be the so-called helifan structures, recently discovered for holmium.[37] The noisy behavior observed under decreasing-field conditions resembles the so-called Barkhausen noise connected with domain structures. Recently, this type of phenomena has been recognized as an example of the self-organized criticality[38] (compare Fig. 11 with Fig. 1 in Ref. 38).

B. Irreversibility behavior inside the fan-phase region

The behavior of the magnetic susceptibility inside the region corresponding to the fan phase was previously reported in Ref. 23. In Secs. V B and V C, the main findings are briefly recapitulated and discussed in relation to some results on the same issue.

A strong irreversibility is found inside the fan region. At a given temperature, the susceptibility measured on increasing field is higher than for the reversed field direction, mentioned already in relation to Figs. 5, 10, and 12. The $\chi'(H)$ curve at 4.2 K, shown in Fig. 14, illustrates this stunning irreversible behavior inside the fan phase and demonstrates also the appearance of the minor hysteresis loops. In Fig. 14 the field was first increased to about 60 kOe, so that the system reached the P phase and then decreased. After initiation of the irreversible behavior (between 40 and 50 kOe), the field was increased and then decreased again in order to form the minor hysteresis loop (5–6 in Fig. 14). This process was then repeated several times and is illustrated by the loops (7–8), (9–10), (11–12), (13–14), and (15–16). The dotted line in Fig. 14 shows a subsequent complete field run up into the P phase and back down to zero field. Besides this hysteresis behavior, it is seen that on decreasing the field, a χ' lower than that obtained with the nonstop decrease of the field may be attained [as evident from the region between (7–8) and (11–12) in Fig. 14]. Another observation in low fields is that values of χ' corresponding to the loop (15–16) can only be obtained on decreasing-field conditions. The hysteresis width inside the fan phase is about 8 kOe roughly throughout the fan phase.

In order to check the long-term behavior of the magnetic state at a given field and temperature inside the fan phase, an experiment was made where the system was brought to the state denoted A in Fig. 14. For the studied 4-h period, the susceptibility remained constant, and no sign of relaxation to the limits of the hysteresis region was observed.

The possibility of thermal hysteresis inside the fan phase was also considered. The field was first fixed at 20.4 kOe, and the temperature was decreased from 60 to 28 K. The P–fan transition appears as a distinct peak in χ'. No anomaly was observed in χ''. Then, at 28 K, the field was increased to 24 kOe and the sample warmed up to about 50 K. While keeping the field at this value, the system was cooled to 28 K. These runs are illustrated by the χ' curves in Fig. 15, where no significant thermal hysteresis is seen (estimated as maximum 0.5 K at the lowest temperature). The overall picture of a lack of a sizable thermal hysteresis is contrary to the huge hysteresis observed when the field was varied.

For the discussion of the strong irreversible behavior inside the fan phase, let us first consider the possibility that the effect originates from domains as normally found for hard ferromagnetic materials. The present sample is a single crystal, which implies that a semimacroscopic mechanism such as a difficulty in reorientation of the **M** vector in monodomain crystallites (which contributes to the irreversible behavior in technical magnets) can be excluded. The pinning centers in a single crystal have, in our opinion, not high enough energy barriers to account for the magnitude (some 10 kOe) of the fields involved in the hysteresis. The inhomogeneities at the atomic level (concerning the distribution of Co atoms) can hardly accommodate such a pinning mechanism.

A more reasonable explanation could be the occurrence of "lock-in"-type phases inside the region corresponding to the fan phase, in which the wave vector **q** is locked at a particular value. In fact, in pure MnP, the **q**

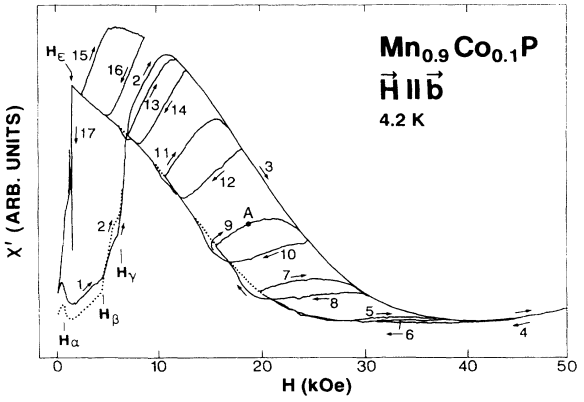

FIG. 14. $\chi'(H)$ in the fan phase (**H**‖**b**) illustrating hysteresis behavior and the onset of irreversibility behavior at high fields. The solid curve shows field sweeps switched up and down (progressively numbered) to produce hysteresis loops. The dashed curve segments indicate the difference of subsequent runs (only up and down in field) from the previous oscillatory run.

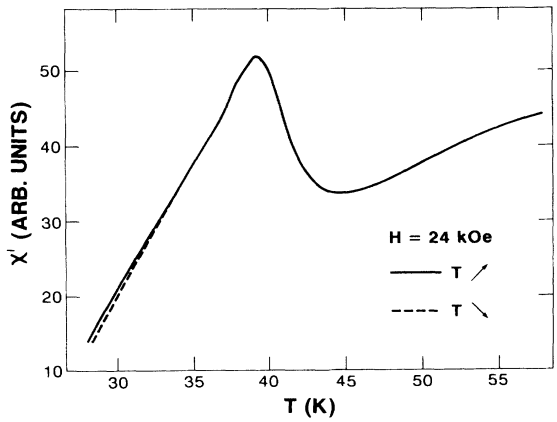

FIG. 15. $\chi'(T)$ at 24 kOe extracted from continuous recordings on increasing and decreasing temperature conditions (solid and dashed line, respectively), after cooling the sample in zero field (**H**‖**b**).

vector of the fan phase is field dependent.[7,19] The $\mathbf{q}(H)$ dependence was studied for powder samples of $Mn_{0.8}Co_{0.2}P$, and the results show a significant field dependence (22% decrease on going from 2 to 12 kOe; see Fig. 13 in Ref. 22). The behavior of the fan phase in pure MnP has previously been discussed[39] in terms of the axial next-nearest-neighbor Ising (ANNNI) model, which considers lock-in phases and commensurate–incommensurate transitions. The unusual magnetic behavior inside the fan phase was there attributed to the possible existence of a sequence of closely spaced first-order commensurate–incommensurate transitions. The present results for $Mn_{0.9}Co_{0.1}P$ favor this kind of interpretation. The lack of a noticeable time dependence is also consistent with the picture of lock-in phases.

Finally, the lack of appreciable thermal hysteresis in field-cooled experiments (Fig. 14) should be noted, which may be due to the weak temperature dependence of the wave vector $\mathbf{q}$ in a given field. In the lock-in phase picture, this will, at least qualitatively, explain the lack of thermal hysteresis since the value of $\mathbf{q}$ (and hence χ) is mainly determined by H. [Measurements for powder samples[22] of $Mn_{0.8}Co_{0.2}P$ show an intriguing weak (some 2%) temperature variation of $\mathbf{q}$ between 10 and 50 K (compared with an 11% decrease for the screw phase of MnP in zero field). This behavior contrasts with the strong field dependence of $\mathbf{q}$, which is illustrated by the fact that the effect of a 1-kOe field corresponds to a 20-K temperature change.] Single-crystal neutron-diffraction data will be of fundamental importance in order to provide an experimental answer to the irreversibility behavior.

C. Fan–*P* transition region: Irreversibility line

The reversible behavior is recovered when the system enters the P phase at high fields. At high temperatures the fan–P transition appears in the $\chi'(H)$ curves as a kink followed by a sharp drop in χ' (see Fig. 5). As the temperature is lowered, the transition field increases and the signature of the second-order fan–P transition becomes less pronounced and disappears below 10 K. The evolution is shown in Fig. 16. Note that the field where irreversibility starts, H_{irr}, is always higher than $H_{\lambda *}$. On further decrease of the temperature down toward 1.7 K, the irreversibility field continues to increase. The method for determination of H_{irr} is discussed in Ref. 23. The resulting phase diagram is shown in Fig. 17.

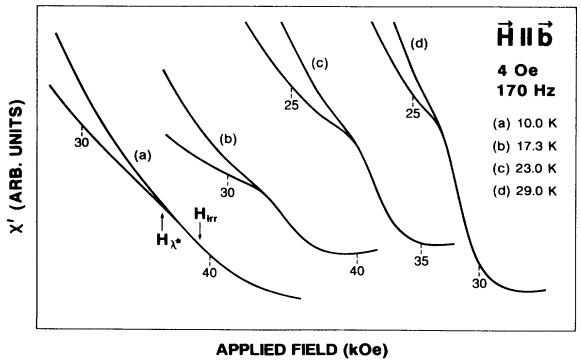

FIG. 16. Selected susceptibility traces $\chi'(H)$ ($\mathbf{H}\|\mathbf{b}$) at temperatures given in the illustration. The curves are shifted horizontally for clarity; field scale markers (in kOe) are given for each curve. Note that for $T=10.0$ K remanence of the $H_{\lambda *}$ kink can still be seen.

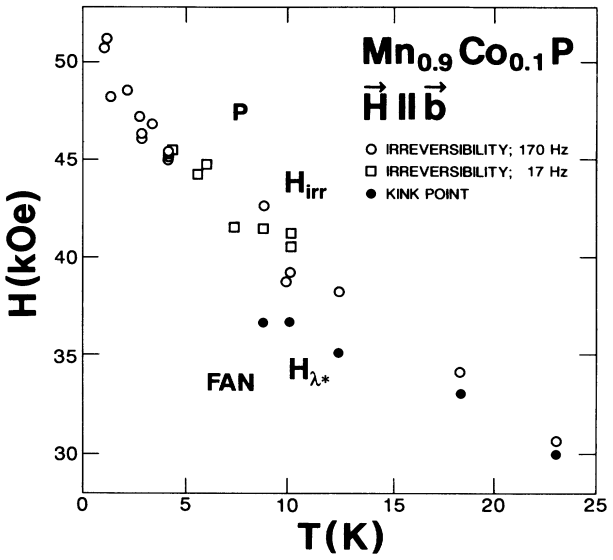

FIG. 17. Low-temperature high-field portion of the magnetic phase diagram for $Mn_{0.9}Co_{0.1}P$ ($\mathbf{H}\|\mathbf{b}$) (from Ref. 23, with a few points added). The legend to the symbols is given in the illustration.

This behavior contrasts with that found in pure MnP where no irreversibility is observed, the second-order transition to the P phase is very sharp, and the transition field approaches a constant value as $T\rightarrow 0$. Note that $H_{\lambda *}$ occurs at almost the same fields for $Mn_{0.9}Co_{0.1}P$ and MnP.

A sharp increase of the irreversibility line as $T\rightarrow 0$ is predicted to occur for the random-field Ising model (RFIM).[8] It is well known that the RFIM is experimentally realized for a diluted antiferromagnet in an external field.[11] The existence of an irreversibility line for a diluted Ising antiferromagnet in field has been confirmed by Monte Carlo simulation.[40] It is possible that the irreversibility-line behavior in $Mn_{0.9}Co_{0.1}P$ is related to the RFIM predictions. However, it is difficult to tell whether an appropriate model for $Mn_{0.9}Co_{0.1}P$ can be put in correspondence with the RFIM. If so, substitutionally diluted MnP will be a convenient experimental system for studying RFIM effects at the $T\rightarrow 0$ limit, since the critical line hits $T=0$ at quite a low field.

ACKNOWLEDGMENTS

This work has received financial support from the Norwegian Council for Science and the Humanities, the Polish Science Programme CPBP 01.12, and the Brazilian Scientific Agencies Fundacão de Amparo a Pesquisa

do Estado de São Paulo (FAPESP) and Conselho Nacional de Desenvolvimento Cientifico e Tecnologico (CNPq). The skillful assistance of S. Lacher, Max Planck Institut für Festkörperforschung, Stuttgart, in the crystal preparation work, and the participation of Z. Lodziana, AGH Krakow, in a pulse-field experiment, is gratefully acknowledged. We also thank A. Aharony and D. Mukamel for valuable comments on LP theory.

[1]C. C. Becerra, Y. Shapira, N. F. Oliveira, Jr. and T. S. Chang, Phys. Rev. Lett. **44**, 1692 (1980).
[2]Y. Shapira, C. C. Becerra, N. F. Oliveira, Jr., and T. S. Chang, Phys. Rev. B **24**, 2780 (1981).
[3]Y. Shapira, N. F. Oliveira, Jr., C. C. Becerra, and S. Foner, Phys. Rev. B **29**, 361 (1984).
[4]R. H. Moon, J. W. Cable, and Y. Shapira, J. Appl. Phys. **52**, 2025 (1981).
[5]V. Bindilatti, Ph.D. thesis, University of São Paulo, 1988.
[6]V. Bindilatti, C. C. Becerra, and N. F. Oliveira, Jr., Phys. Rev. B **40**, 9412 (1989).
[7]C. C. Becerra, V. Bindilatti, and N. F. Oliveira, Jr., in *New Trends in Magnetism,* edited by M. Coutinho and S. Rezende (World Scientific, Singapore, 1990).
[8]S. Fishman and A. Aharony, J. Phys. C **12**, L729 (1979); D. S. Fisher, G. M. Grinstein, and A. Khurana, Phys. Today **41**(12), 56 (1988), and references therein.
[9]A. Paduan-Filho, Y. Ridente, S. Zacarelli, and C. C. Becerra, J. Phys. (Paris) Colloq. **49**, Suppl. **12**, C8-823 (1988).
[10]J. Wosnitza and H. v. Lohneysen, Europhys. Lett. **10**, 381 (1990).
[11]R. J. Birgenau, R. A. Cowley, G. Shirane, and H. Yoshizawa, Phys. Rev. Lett. **54**, 2147 (1985).
[12]D. P. Belanger, A. R. King, and V. Jaccarino, Phys. Rev. Lett. **54**, 577 (1985).
[13]E. E. Huber, Jr. and D. H. Ridgley, Phys. Rev. **135**, A1033 (1964).
[14]P. G. Felcher, J. Appl. Phys. **37**, 1056 (1966); J. B. Forsyth, J. S. Pickart, and P. J. Brown, Proc. Phys. Soc. London **88**, 33 (1966).
[15]R. M. Moon, J. Appl. Phys. **53**, 1956 (1982).
[16]H. Terui, T. Komatsubara, and E. Hirahara, J. Phys. Soc. Jpn. **38**, 383 (1975).
[17]C. C. Becerra, N. F. Oliveira, Jr., and A. C. Migliano, J. Appl. Phys. **63**, 3092 (1988).
[18]H. J. Brumatto, C. C. Becerra, and N. F. Oliveira, Jr., in Proceedings of the 35th Annual Conference on Magnetism and Magnetic Materials, San Diego, 1990; J. Appl. Phys. **69**, 5815 (1991).
[19]A. Takase and T. Kasuya, J. Phys. Soc. Jpn. **47**, 491 (1979).
[20]H. Fjellvåg, A. Kjekshus, A. Zięba, and S. Foner, J. Phys. Chem. Solids **45**, 709 (1984).
[21]A. Zięba, H. Fjellvåg, and A. Kjekshus, J. Phys. Chem. Solids **49**, 1087 (1988).
[22]H. Fjellvåg and A. Kjekshus, Acta Chem. Scand. A **38**, 563 (1984).
[23]C. C. Becerra, A. Zięba, N. F. Oliveira, Jr., and H. Fjellvåg, J. Appl. Phys. **67**, 5442 (1990).
[24]A. Zięba, C. C. Becerra, N. F. Oliveira, Jr., H. Fjellvåg, and A. Kjekshus, J. Magn. Magn. Mater. **104-107**, 71 (1992).
[25]C. C. Becerra *et al.* (unpublished).
[26]H. Fjellvåg, A Kjekshus, and A. Zięba, Acta Chem. Scand. A **44**, 8 (1990).
[27]Z. Lodziana, M.E. thesis, AGH, Krakow, 1991.
[28]M. E. Fisher, Am. Inst. Phys. Conf. Proceedings **24**, 273 (1975).
[29]A. Zięba (unpublished).
[30]R. M. Horneich, M. Luban, and S. Shtrikman, Phys. Rev. Lett. **35**, 1678 (1975). For a review of LP theory, see R. M. Hornreich, J. Magn. Magn. Mater. **15-18**, 387 (1980).
[31]A. B. Harris, J. Phys. C **7**, 1671 (1974); see also T. C. Lubensky, Phys. Rev. B **11**, 3573 (1975).
[32]A. Aharony and D. Mukamel (private communication): $\alpha_{rL} = -A(4.5-d)^{1/2} + O(4.5-d)$, where A is an unknown positive constant.
[33]C. S. O. Yokoi, M. D. Coutinho-Filho, and S. R. Salinas, Phys. Rev. B **29**, 6341 (1984).
[34]A. Michelson, Phys. Rev. B **16**, 577 (1977) (see Appendix B).
[35]A. Paduan-Filho, C. C. Becerra, and F. Palacio, Phys. Rev. B **43**, 11 107 (1991).
[36]A. Paduan-Filho, C. C. Becerra, C. Westphal, M. Gabas, and F. Palacio, J. Magn. Magn. Mater. **104-107**, 269 (1992).
[37]J. Jensen and A. R. Mackintosh, Phys. Rev. Lett. **64**, 2699 (1990).
[38]P. J. Cote and L. V. Meisel, Phys. Rev. Lett. **67**, 1334 (1991).
[39]C. C. Becerra, N. F. Oliveira, Jr., and Y. Shapira, J. Phys. (Paris) Colloq. **49**, Suppl. 12, C8-895 (1988).
[40]K. D. Usadel and U. Nowak, J. Magn. Magn. Mater. **104-107**, 179 (1992); U. Nowak and K. D. Usadel, Phys. Rev. B **44**, 7426 (1991).

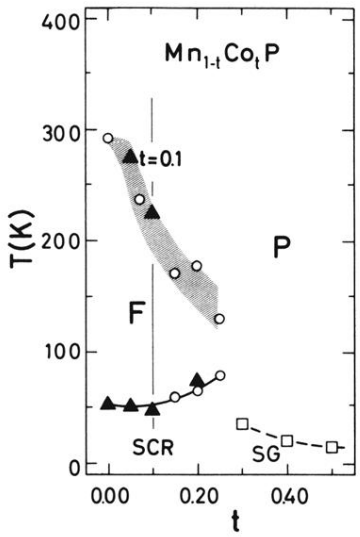

FIG. 2. Temperature–composition phase diagram for polycrystalline $Mn_{1-t}Co_tP$ (from Ref. 20). SG denotes the spin-glass region.